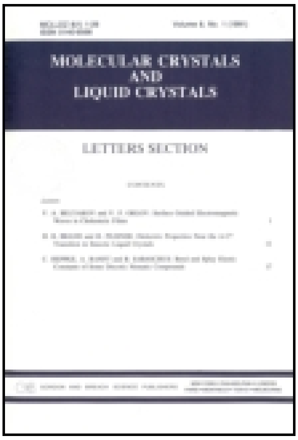

Molecular Crystals and Liquid Crystals
Publication details, including instructions for authors and subscription information:
http://www.tandfonline.com/loi/gmcl20

Low Frequency Noise Characteristics on Al/Nb_2O_5/p-type Schottky Diode Fabricated by Pulsed DC Magnetron Sputtering

Hyun Gon Oh [a], Kyung Soo Kim [a], Jimi Eom [b], Sang Jik Kwon [b], Eou Sik Cho [b], Jong-Ho Lee [c] & Il Hwan Cho [a]

[a] Department of Electronic Engineering, Myongji University, Yongin, Gyeonggi, 449-728, Republic of Korea

[b] Department of Electronic Engineering, Gachon University, Seongnam, 461-701, Republic of Korea

[c] School of Electronic Engineering and Computer Science, Seoul National University, Seoul, 151-742, Republic of Korea

Published online: 08 Jan 2014.

To cite this article: Hyun Gon Oh, Kyung Soo Kim, Jimi Eom, Sang Jik Kwon, Eou Sik Cho, Jong-Ho Lee & Il Hwan Cho (2013) Low Frequency Noise Characteristics on Al/Nb_2O_5/p-type Schottky Diode Fabricated by Pulsed DC Magnetron Sputtering, Molecular Crystals and Liquid Crystals, 586:1, 168-178, DOI: 10.1080/15421406.2013.853551

To link to this article: http://dx.doi.org/10.1080/15421406.2013.853551

Mol. Cryst. Liq. Cryst., Vol. 586: pp. 168–178, 2013

ISSN: 1542-1406 print/1563-5287 online
DOI: 10.1080/15421406.2013.853551

Low Frequency Noise Characteristics on Al/Nb_2O_5/p-type Schottky Diode Fabricated by Pulsed DC Magnetron Sputtering

HYUN GON OH,[1] KYUNG SOO KIM,[1] JIMI EOM,[2] SANG JIK KWON,[2] EOU SIK CHO,[2] JONG-HO LEE,[3] AND IL HWAN CHO[1,*]

[1]Department of Electronic Engineering, Myongji University, Yongin, Gyeonggi, 449-728, Republic of Korea
[2]Department of Electronic Engineering, Gachon University, Seongnam 461-701, Republic of Korea
[3]School of Electronic Engineering and Computer Science, Seoul National University, Seoul 151-742, Republic of Korea

Nb_2O_5 films were deposited with pulsed DC magnetron sputter which is versatile and provides the ability to deposit thin film of oxide compounds with high deposition rate. Current measurement data from the metal-insulator-semiconductor (MIS) structure followed Schottky emission mechanism andreverse current characteristics were analyzed with oxygen flow rate variation. Low frequency noise measurements have been carried out with MIS samples at the forward conduction region. The experimental noise data have been successfully explained by the random walk model. The effect of O_2 flow rate of deposition process on low frequency noise has also been investigated and analyzed.

Keywords DC pulsed sputtering; dielectric material; low frequency noise; niobium oxide

Introduction

Niobium oxides demonstrate a broad range of electrical properties, which vary from dielectric for Nb_2O_5 to semiconducting for NbO_2 and to metallic for NbO [1]. Nb_2O_5 film are used in electrolytic capacitors with polyaniline/polypyrrole as cathode material. [2] Nb_2O_5 such as the transition metal oxides is utilized in gas sensors, catalysis, optical and electrochromic devices [3–5].

The Nb_2O_5 films can be prepared by variety of techniques. In order to form the Nb_2O_5 films, such as anodic oxidation [6], thermal growth [7], pulsed layer deposition (PLD) [8] orradio frequency (RF) sputtering [9] can be used. Within the various fabrication processes, pulsed-DC magnetron sputtering is versatile and provides an ability to deposit thin film of oxide compounds with high deposition rate compared to the RF magnetron sputtering

*Address correspondence to Prof. Il Hwan Cho, 3rd Eng. Building Room 19401, Department of Electronic Engineering Myongji University, Nam-dong, Cheoin-gu, Yongin, Gyeonggi, 449-728 Korea (ROK). Tel.: (+82)31-330-6380; Fax: (+82)31-330-6975. E-mail: ihcho77@mju.ac.kr

Table 1. Sputtering process conditions of Nb_2O_5 film

Sputtering method target	Pulsed DC Nb_2O_5 target
Power [W]	300
Pulse Freq [kHz]	200
Reverse time [μs]	1.5
Pressure [mTorr]	6
Ar flow rate [sccm]	50
O_2 flow rate [sccm]	1, 1.5, 2, 2.5
Jig moving speed [Hz]	10
Base vacuum	2×10^{-6}
Temperature [°C]	R. T

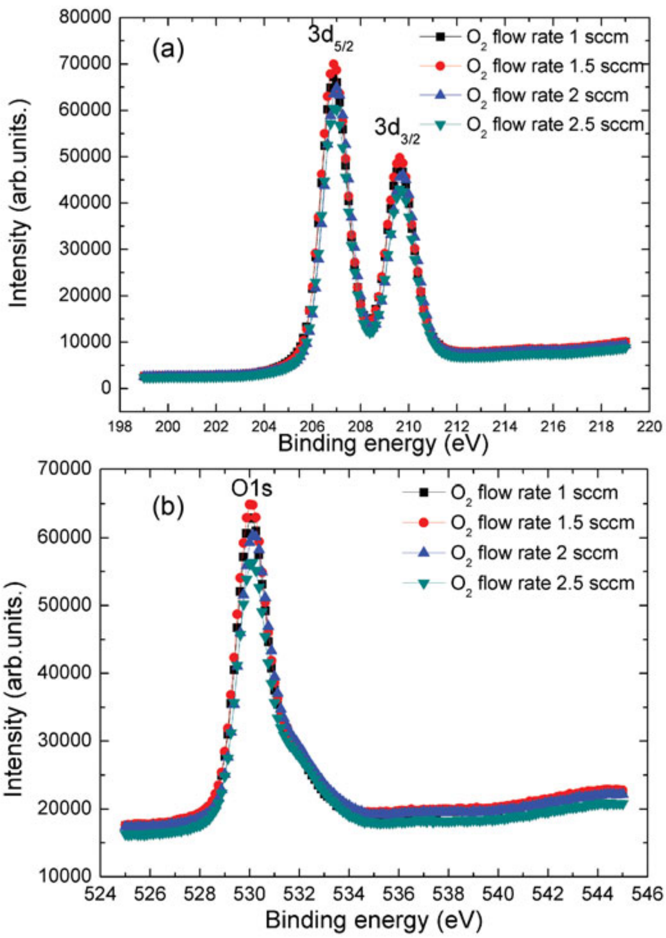

Figure 1. Nb_2O_5 film XPS core-level spectra of Nb_2O_5 film (a) core level of Nb^{5+} ion. (b) core level of O^{2-} ion.

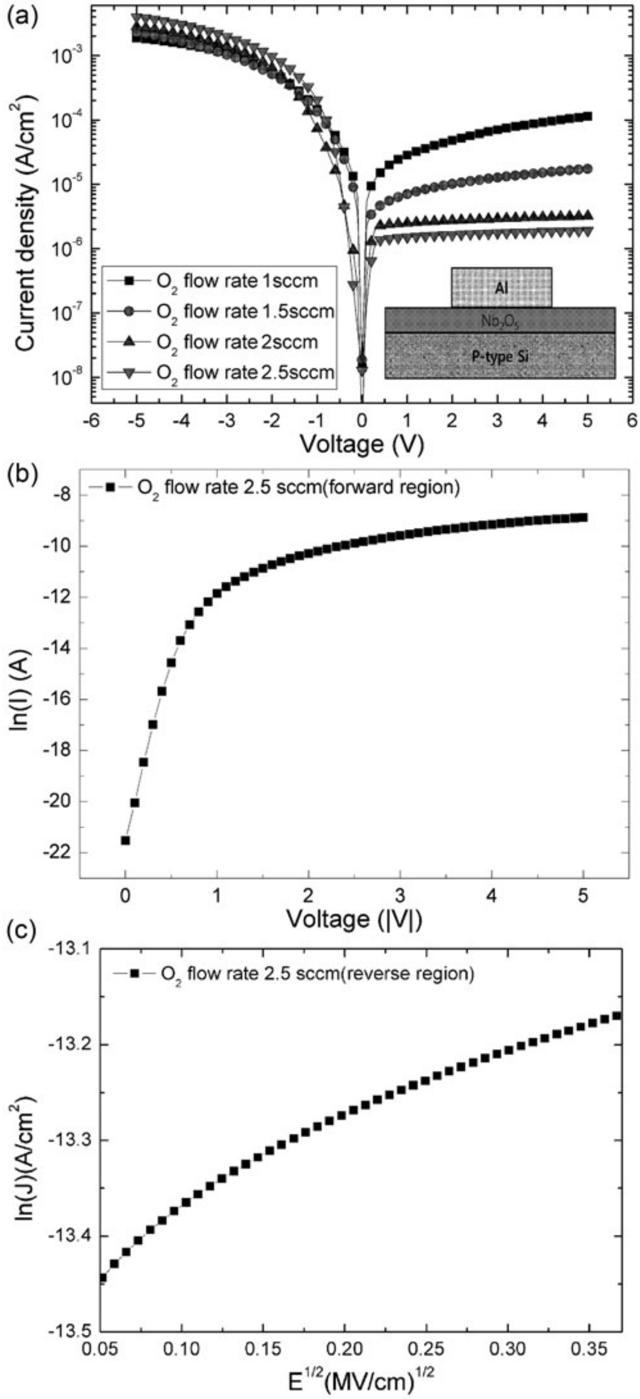

Figure 2. Electrical current characteristics of MIS diode with Nb_2O_5 (a) I-V characteristics with O_2 flow rate (b) ln(I) vs V plot in forward bias region (c) ln(J) vs $E^{1/2}$ plot in reverse bias region.

Table 2. Barrier height and chemical composition of Nb_2O_5 film with O_2 flow rate variation

O_2 flow rate (sccm)	Thickness (nm)	Barrier height (eV)	Chemical composition (O:Nb)
1	160.31	0.58	2.75
1.5	142.43	0.62	2.79
2	93.10	0.64	2.87
2.5	68.16	0.65	2.9

methods. Also, it has long-term stability, low arcing characteristic and low number of defect for the deposition of a dielectric thin film [10,11]. In this work, Nb_2O_5 films are deposited at room temperature from Nb_2O_5 target using a pulsed-DC magnetron sputtering. The room temperature fabrication of Nb_2O_5 film is able to apply about a flexible substrate.

Major advantages for all these applications are the long term stability and an acceptable level of the low frequency noise. Noise analysis can be used as a diagnostic tool for improving device performance and obtaining substantial information on the physical properties of the Nb_2O_5 material.

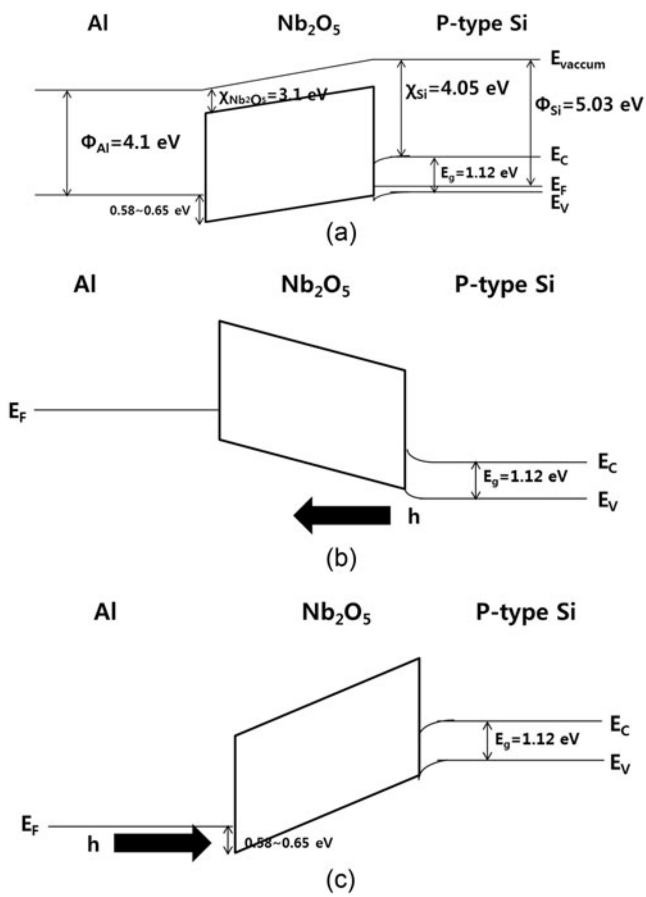

Figure 3. Energy band diagram of MIS structure (a) zero bias region (b) forward bias region (c) reverse bias region.

The low frequency noise characteristic of Nb_2O_5 films were widely analyzed with reactive magnetron sputtering [12], PLD [13] and RF sputtering [14].

In this paper, we investigate current-voltage (I-V) characteristicsand low frequency noise characteristic of Al/Nb_2O_5/P-type silicon MIS structureby using a pulsed-DC magnetron sputtering. We also investigate the effect of O_2 flow rate on low frequency noise characteristics.

Experimental

MIS diodes are fabricated on p-type silicon wafer (100). After surface cleaning, Nb_2O_5 filmis deposited on p-type substrate with pulsed-DC magnetron sputtering. Sputtering process was performed at room temperature with a constant power of 300 W. The applied bias is changed with a frequency of 200 kHz and 1.5 μs reverse time to avoid charge accumulation and arcing. O_2 flow rate is varied from 1.0 sccm to 2.5 sccm. The thickness of Nb_2O_5 film is varied in accordance with O_2 flow rate. Table 1 shows process conditions of sputtering. After deposition process, Nb_2O_5 film is annealed in a forming gas ambient at 400 °C. For the measurement, 400 nm-thick Al top electrodes with an area of $351\times 10^4 \mu m^2$ are formed using pulsed-DC magnetron sputtering and then do the lift-off method.

I-V characteristics are measured with a semiconductor parameter analyzer (Hewlett-Packard, 4156A). The low frequencynoise is measured at the forward region of operation using a SR570 low noise amplifier and dynamic signal analyzer (Agilent 35670A) for frequency spectrum. The bias is applied by CdNi batteries to avoid any external LF noise.

Results and Discussion

All of Nb_2O_5 films in this work have amorphous phase because the process temperature is lower than 400 °C [15].

Binding energies of Nb-3d level have 209.62 eV in Nb3d3/2 and 206.87 eV in Nb3d5/2 respectively. The O1s level binding energy of oxygen has 530 eV. And near peak 532 eV can be explained as the binding energy assigned to the oxygen (O^{2-}) anion in surface oxygen [16]. All of the binding energies in the sample are equal in terms of the measurement data in previous work [16].

However, O_2 flow rate variation has no effect on binding energy of Nb_2O_5. Figure 1 shows Nb_2O_5 layer which is deposited by pulsed-DC magnetron sputteringwith Nb_2O_5 target. It also has same atomic structure with Nb_2O_5 layer of previous work. Figure 2 illustrates the plot of electrical current versus gate voltage. As shown in Fig. 2(a), electrical currents were affected by O_2 flow rate. To identify the conduction mechanism of the Nb_2O_5 films, logI (current) versus V (voltage) of Nb_2O_5 film with 2.5 sccm O_2 flow rate was plotted in forward (negative) bias region, as shown in Fig. 2(b). The current characteristics followed Schottky emission. In the lowvoltage region, log I was linear with V and the slope was changed with voltage increase.

As shown in Schottky-emission equation (1), the change of slope is responsible for the voltage drop with series resistance.

$$I = I_o \exp\left(\frac{q\,(V - IR_s)}{nkT}\right)\left[1 - \exp\left(-\frac{q\,(V - IR_s)}{kT}\right)\right] \qquad (1)$$

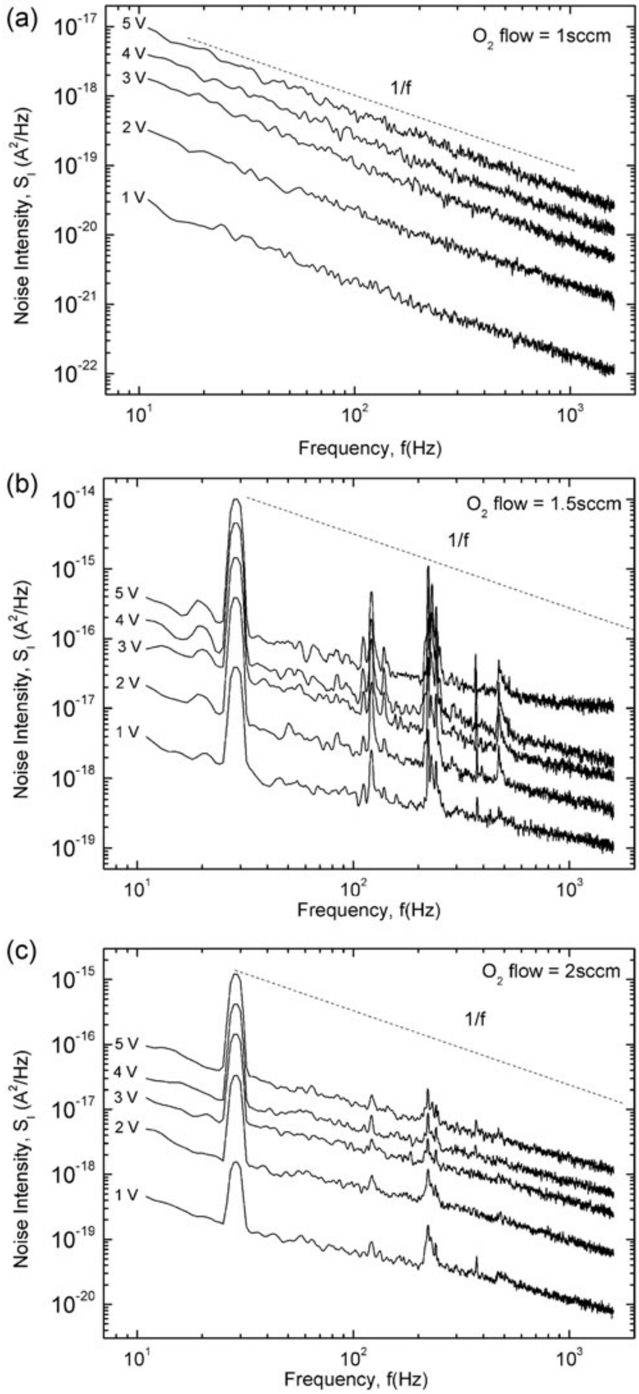

Figure 4. Spectral current density S_I versus frequency on the Al/ Nb_2O_5/p-Si MIS diode. It is measured with different forward bias $V_F = -1, -2, -3, -4$, and -5 V. (a) 1 sccm, (b) 1.5 sccm, (c) 2 sccm, (d) 2.5 sccm. *(Continued)*

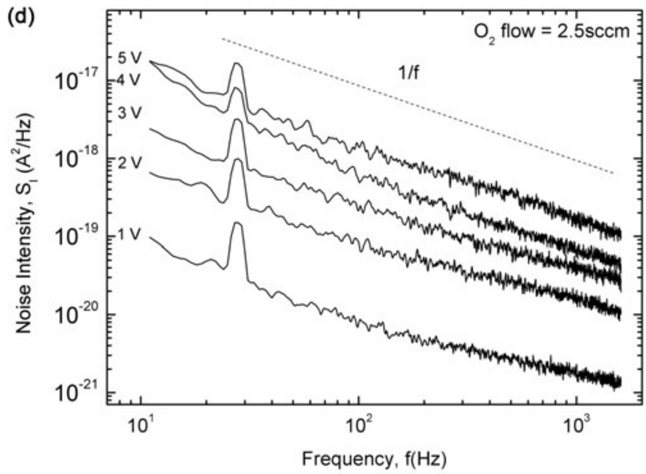

Figure 4. *(Continued)*

Where q is the electronic charge, n is the ideality factor, R_S is the series resistance, *k* is the Boltzmann constant and I_o is the saturation current [17].

Figure 2(c) shows reverse region current characteristics of MIS structure.In the reverse region, lnJ (current density) vs $E^{1/2}$(electric field) plot has linear relationship. This is responsible for saturation current characteristics of Schottky emission [18]. Investigation of electrical characteristics indicated that the current conduction mechanism is Schottky emission.

O_2 flow rate dependency of Nb_2O_5 film with pulsed DC magnetron sputtering is investigated with material properties of film. According to the data in table 2, the thickness of Nb_2O_5 is decrease as O_2 flow rate increases. However the reverse region current is decreased as O_2 flow rate increases and this relationship indicates that the current is not determined by the Ohmic conduction. Considering the barrier height and work function of each material, energy band diagrams of MIS structure were estimated as shown in Fig. 3. As shown in the energy band diagram, reverse currents were mainly determined by barrier height and this can be proved by reverse saturation current equation as shown in equation (2) [19].

$$I_o = AA^*T^2 \exp\left(-\frac{q\O_B}{KT}\right) \tag{2}$$

In the Eq. (2), A is the area of rectifier contact, A^* is the effective Richardson constant and equals to 32 $Acm^{-2}K^{-2}$ for p-Si,*k* is the Boltzmann constantand Φ_B is the barrier height.

Figure 4 shows noise spectrum of the MIS diode with different forward bias ($V_F = -1, -2, -3, -4$, and -5V). The 1/f behavior is apparently shown in all the investigated frequency range. The result of a pure 1/f noise indicates the uniformity in the energy distribution of trapping state [20].

The most of visible activity in this field is definitely the ubiquitous 1/f noise. The 1/f noise arises, because large classes of fluctuations in condensed matter system. It is shown a power spectrum (S(f)) that has $1/f^{\alpha}$ frequency dependence with $\alpha \sim 1$ [21].

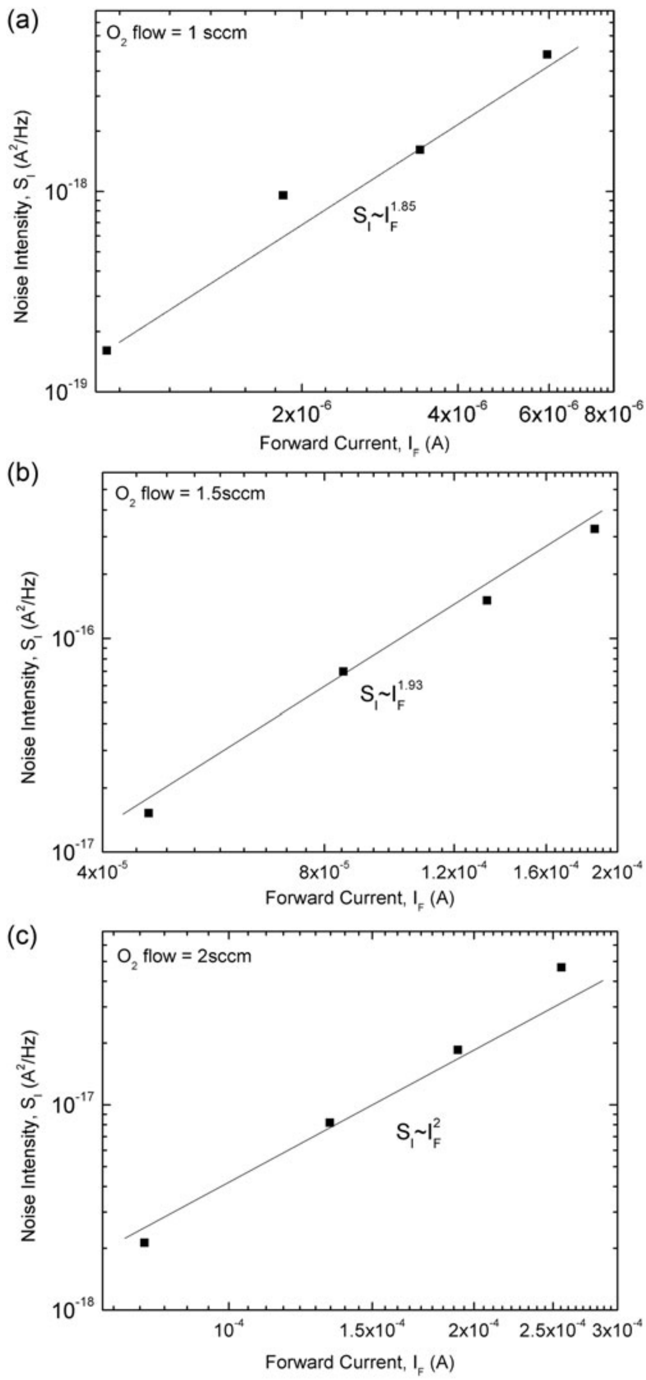

Figure 5. The relation of noise intensity and the forward current on the Al/ Nb_2O_5/p-Si MIS diode (a) 1 sccm, (b) 1.5sccm, (c) 2 sccm, (d) 2.5 sccm. *(Continued)*

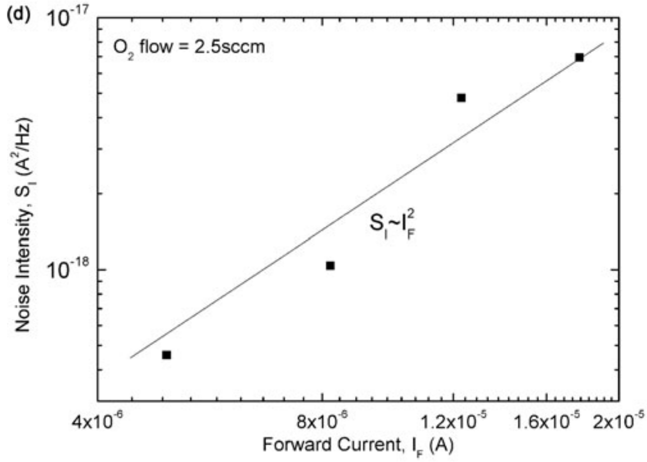

Figure 5. *(Continued)*

In 1/f noise source [22], it is impossible to obtain a distribution of the thermal activation energy from trap levels in the energy gap of the semiconductor. Simply, traps of a few kT below and above the Fermi level contribute to the noise. The spectrum result would be the sum of two smeared-out Lorentzians and the electron transition from the conduction band to the valence band. A similar argument is given by Hooge. The Dutta-Horn model of thermal activation in which a peak of energy values a few kT wide is sufficient to produce a 1/f type or $1/f^{\alpha}$ spectrum. Thus, it can not be applied to trap levels in semiconductors. But it might be applied to mobility fluctuation at low temperatures [20].

The current noise spectral density S_I is measured at constant frequency f = 20 Hz. Figure 5 shows power spectral density S_I and forward current I_F relation. The relationship is expressed in equation (3) [23].

$$S_I(f) \propto \frac{I_F^{\beta}}{f} \tag{3}$$

Where β means the slope of S_I, f is the frequency. It is shown that β equals 2 in 2 sccm of O_2 flow and 2.5 sccm of O_2 flow as shown in Figs. 5(c) and (d).

The noise intensity due to the random walk model of electrons at the interface is obtained as a function of the interface states density as follows [12],

$$S_I = \frac{G}{f}\left(\frac{qI_F}{4\varepsilon}\right)^2 \frac{q^2 D_{it}}{\pi\, k\, T\, N_d\, W\, A} \tag{4}$$

In Eq. (4), G is the distribution constant of time constant given by the random walk model. G is equal to 0.1 [24]. N_d, and ε are the doping concentration and permittivity of Si, W is the width of the depletion region, A is the area of the diode, kT is the thermal energy, and D_{it} is the interface states density.

The random walk model for electrons at the interface states has been known to generate 1/f noise in semiconductor devices. The random walk model is applied by Jantsch [24] to explain for the 1/f noise in Schottky barrier diodes, where he studied the fluctuation of the surface generation-recombination current which is directly related to the fluctuation in the occupancy of the interface state in accordance with the generation-recombination theory of diodes [20].

However, slopes of Figs. 5(a) and (b) are slightly smaller then 2. That can be explained by inhomogeneity of the barrier height at the surface [23]. From this result, O_2 flow rate of Nb_2O_5 films can modulate barrier height uniformity at the surface.

Conclusions

We investigated the I-V and low frequency noise characteristic of Al/Nb_2O_5/p-Si MIS diode fabricated via pulsed DC magnetron sputtering with different O_2 flow rate. The I-Vcharacteristics of Al/ Nb_2O_5/p-Si MIS diode followthe Schottky emission characteristic. At forward bias, the power spectral density appearing in Al/Nb_2O_5/p-Si MIS diode shows a 1/f noise and is proportional to I^2. In the results of low frequency noise measurements, we found that low frequency noise characteristics of MIS diode satisfy the random walk model with the increasing of O_2 flow rate. The deviation of the values of $\beta(= 2)$ is explained by the random walk of electrons involving the Schottky-barrier interface via barrier-height modulation.

Acknowledgments

This research was supported by Basic Science Research Program through the National Research Foundation of Korea (NRF) funded by the Ministry of Education, Science and Technology (2012-0003891).

References

[1] Ye, Z., Zhengjun, Z., & Yuanhua, L. (2004). *J. Phys. D: Appl. Phys.*, *37*, 3392.
[2] Poopathy, K., & Seenivasagan, R. (1995). *Synth. Met.*, *74*, 165.
[3] Mary, E., Gimon, K., & Kenneth, J. B. (1999). *Microporous Mesoporous Mater.*, *28*, 113.
[4] Toshiro, M., & Susumu, A. (1993). *Appl. Phys. Lett.*, *63*, 869.
[5] Richter, F., Kupfer, H., Schlott, P., Gessner, T., & Kaufmann, C. (2001). *Thin Solid Films*, *389*, 278.
[6] Desa, A. I., Rangel, C. M., Skeldon, P., & Thompson, G. E. (2006). *Port. Electrochim. Acta*, *24*, 305.
[7] Logacheva, V. A., Divakova, N. A., & Tikhonova, Y. A. (2007). *Inorg. Mater.*, *43*, 1230.
[8] Jung, K. H., Kim, Y. M., Park, Y. S., Jung, W., & Choi, J. G. (2011). *J. Appl. Phys.*, *109*, 054511.
[9] Zhu, X. H., Defay, E., Suhm, A., Fribourg-blanc, E., & Aid, M. (2009). *Appl. Phys. Lett.*, *94*, 122906.
[10] Arell, R. D., & Kelly, P. J. (1999). *Sur. Coat. Technol.*, *112*, 170.
[11] An, S., In, J., & Chang, H. (2009). *Plasma. Process. Polym.*, *6*, 855.
[12] Lee, J. I., Brini, J., Kamarinos, G., Dimitriadis, C. A., Logothetidis, S., & Patsalas, P. (1999). *Appl. Surf. Sci.*, *142*, 390.
[13] Schmauder, T., Waldauf, A., Wald, H., & Seidel, P. (2000). *Physica. C*, *333*, 23.
[14] Jevtic, M. M., Jelenkovic, E. V., Tong, K. Y., & Pang, G. K. H. (2006). *Thin Solid Films*, *496*, 214.
[15] Ko, E. I. (1990). *Catal. Today*, *8*, 27.
[16] Viet, A. L., Reddy, M. V., Jose, R. B., Chowdari, V. R., & Ramakrishna, S. (2010). *J. Phys. Chem. C*, *114*, 664.
[17] Mustafa, O., & Fahrettin, Y. (2008). *Microelectron. Eng.*, *85*, 646.

[18] Chakraborty, S. (2005). *Microelectron. Eng.*, *81*, 188.
[19] Tataroglu, A., & Altmdal, S. (2008). *Microelectron. Eng.*, *85*, 233.
[20] Lee, J. I., Brini, J., Chovet, A., & Dimitriadis, C. A. (1999). *Solid-State Electron.*, *43*, 2181.
[21] Raychaudhuri, A. K. (2002). *Curr. Opin. Solid State Mater. Sci.*, *6*, 67.
[22] Hooge, F. N. (1994). *IEEE Trans. Electron. Devices*, *41*, 11.
[23] Papatzika, S., Hastas, N. A., Angelis, C. T., & Dimitriadis, C. A. (2002). *Appl. Phys. Lett.*, *80*, 8.
[24] Ottomar, J. (1987). *IEEE Trans. Electron. Devices*, *ED-34*, 5.